Narrow-linewidth megahertz-repetition-rate optical parametric oscillator for high-speed flow and combustion diagnostics

Naibo Jiang,[1] Walter R. Lempert,[1,*] Gary L. Switzer,[2] Terrence R. Meyer,[3] and James R. Gord[4]

[1]Departments of Mechanical Engineering and Chemistry, The Ohio State University, Columbus, Ohio 43202, USA
[2]Innovative Scientific Solutions, Inc., 2766 Indian Ripple Road, Dayton, Ohio 45440, USA
[3]Department of Mechanical Engineering, Iowa State University, Ames Iowa 50011, USA
[4]Air Force Research Laboratory, Propulsion Directorate, Wright-Patterson AFB, Ohio 45433, USA

*Corresponding author: lempert.1@osu.edu

Received 12 September 2007; accepted 27 October 2007;
posted 8 November 2007 (Doc. ID 87467); published 20 December 2007

We demonstrate the ability to generate ultra-high-frequency sequences of broadly wavelength-tunable, high-intensity laser pulses using a custom-built optical parametric oscillator pumped by the third-harmonic output of a "burst-mode" Nd:YAG laser. Burst sequences consisting of 6–10 pulses separated in time by 6–10 μs are obtained, with average total conversion efficiency from the 355 nm pump to the near-IR signal and idler wavelengths of ~33%. Typical individual pulse output energy for the signal and idler beams is in the range of 4–6 mJ, limited by the available pump energy. Line narrowing is demonstrated by means of injection seeding the idler wave using a low-power external-cavity diode laser at 827 nm. It is shown that seeding reduces the time-averaged linewidth of both the signal and idler outputs to ~300 MHz, which is near the 220 MHz Fourier transform limit. Line narrowing is achieved without recourse to active cavity stabilization.

OCIS codes: 190.4970, 280.2490, 280.1740.

1. Introduction

While there has been enormous progress in recent years in the development and application of a variety of optical diagnostic imaging techniques, the ability to capture time-evolving or volumetric information is severely constrained by limitations of available laser technology. Over the last several years, we have been developing the capability of generating "trains" of 20–30 high-energy Nd:YAG pulses, separated in time by a variable period as short as 1 μm [1,2]. The approach utilizes a low-power (order milliwatt), continuous-wave (cw) master oscillator, a custom dual Pockels cell pulse "slicer," and a series of flashlamp-pumped amplifiers. In general, it is found that significant energy pulses can be extracted for sequences as long as ~150 μs, with total energy per burst sequence of ~1.5 J at the fundamental wavelength of 1064 nm, and second- and third-harmonic conversion efficiencies of approximately 50% and 40%, respectively [1]. The burst sequence is repeatable at repetition rates as high as 5–10 Hz, limited by thermal gradients in the flashlamp-pumped amplifiers, which leads to degradation of the spatial beam quality. For all measurements reported in this paper, the laser system was operated at a burst repetition rate of 5 Hz.

In this paper we demonstrate the ability to generate trains of wavelength-tunable pulses using a custom-built optical parametric oscillator (OPO), which is the first step toward our goal of developing an ultra-high-frame-rate planar laser-induced fluorescence (PLIF) imaging system. PLIF is a powerful diagnostic technique that has been widely employed for studies of combustion and high-speed reacting flow [3]. In particular, the immediate motivation of this work are planned measurements, which will employ ultra-high-frame-rate nitric oxide (NO) PLIF imaging for study of the dynamics of unsteady and

0003-6935/08/010064-08$15.00/0

Report Documentation Page

Form Approved
OMB No. 0704-0188

1. REPORT DATE	2. REPORT TYPE	3. DATES COVERED
12 SEP 2007		**00-00-2007 to 00-00-2007**

4. TITLE AND SUBTITLE	5a. CONTRACT NUMBER
Narrow-linewidth megahertz-repetition-rate optical parametric oscillator for high-speed flow and combustion diagnostics	5b. GRANT NUMBER
	5c. PROGRAM ELEMENT NUMBER
6. AUTHOR(S)	5d. PROJECT NUMBER
	5e. TASK NUMBER
	5f. WORK UNIT NUMBER
7. PERFORMING ORGANIZATION NAME(S) AND ADDRESS(ES) **Ohio State University,Department of Mechanical Engineering,Columbus,OH,43210**	8. PERFORMING ORGANIZATION REPORT NUMBER
9. SPONSORING/MONITORING AGENCY NAME(S) AND ADDRESS(ES)	10. SPONSOR/MONITOR'S ACRONYM(S)
	11. SPONSOR/MONITOR'S REPORT NUMBER(S)

12. DISTRIBUTION/AVAILABILITY STATEMENT
Approved for public release; distribution unlimited

13. SUPPLEMENTARY NOTES

14. ABSTRACT

15. SUBJECT TERMS

16. SECURITY CLASSIFICATION OF:			17. LIMITATION OF ABSTRACT	18. NUMBER OF PAGES	19a. NAME OF RESPONSIBLE PERSON
a. REPORT **unclassified**	b. ABSTRACT **unclassified**	c. THIS PAGE **unclassified**	**Same as Report (SAR)**	**8**	

turbulent flow behavior in a hypersonic Mach 10 wind tunnel [4], including, potentially, quantitative velocity measurements using NO molecular tagging velocimetry [5]. Since PLIF is based on resonant absorption of radiation, high-instantaneous-power, wavelength-tunable laser sources are required for time-resolved imaging. While dye and/or solid-state sources, including Nd:YAG-pumped OPOs, are readily available commercially, the published technology on generation of high-speed bursts of such tunable radiation is, to our knowledge, limited to three papers. Wu *et al*. [6] pumped a grazing-incidence dye laser with ~0.5 mJ per pulse at 532 nm from an Nd:YAG burst-mode laser similar to that used in the present work. While burst-mode output was obtained, the individual pulse energies were too low to be measured. Luff *et al*. [7] have reported an alexandrite system, which utilizes the combination of a long-pulse (~170 ns) *Q*-switched oscillator, a Harriott cell regenerative amplifier (for pulse slicing and amplification), and two single-pass amplifiers. Approximately 150 μJ per pulse for a 30 pulse sequence with 1 μs separation at 761 nm was reported. Kaminski *et al*. [8] used a set of four commercial double-pulsed Nd:YAG lasers to pump a single commercial dye laser. Starting with 270 mJ per individual pulse at 532 nm, they were able to generate eight pulses at 282 nm, with an average energy of ~1 mJ and a minimum interpulse period of 125 μs, constrained by the high-intensity pumping requirement of the dye laser.

Our strategy is to utilize an OPO for the generation of tunable radiation, taking advantage of the fact that the gain essentially decays instantaneously after the passage of each pump pulse within the burst. It was hypothesized that photobleaching effects, which severely limit the repetition rate of dye lasers, would therefore be minimal, as would be thermal effects since absorption in β-barium borate (BBO) at 355 nm is quite low [9]. As will be shown, this approach enables trains of ~6–10, 5 ns duration pulses, with an individual signal/idler pulse energy of ~4–6 mJ each, limited only by the available 355 nm pump energy. Typical interpulse spacing is between 6 and 10 μs, limited at the current time by the amplitude envelope of the Nd:YAG pump source.

We also demonstrate that the spectral linewidth of both the signal and idler waves can be reduced to ~300 MHz by injection seeding with a low-power cw external-cavity diode laser [10–12]. Furthermore we show that the use of a low-finesse cavity enables narrow-linewidth operation without the need for active cavity stabilization.

2. Experiment

The burst-mode Nd:YAG pump laser, based on a design originally presented by Wu *et al*. [2], has been described in detail previously [1] and will only be very briefly summarized here. A cw Nd:YAG ring laser serves as the primary oscillator, the output of which is preamplified in a double-pass, flashlamp-pumped, pulsed amplifier. The resulting ~150 μs duration pulse is formed into a "burst" train using a custom, dual Pockels cell slicer. The output of the slicer is further amplified in a series of four additional amplifiers and then wavelength converted to either the second-harmonic wavelength (532 nm) with a type II KTP second-harmonic generation (SHG) crystal, or to the third-harmonic wavelength (355 nm) using a pair of type I lithium triborate (LBO) crystals, as described by Dergachev *et al*. [13]. As described in detail recently [1] a phase conjugate mirror (PCM), similar to that which has been employed in pulsed dye lasers [14] to remove amplified spontaneous emission (ASE), is inserted between the third and fourth amplifiers, the purpose of which is to eliminate a low-intensity pedestal resulting from finite on/off contrast of the pulse slicer, and to suppress ASE growth in the forward direction. The final output is a flexible burst of pulses, with interpulse spacing as short as 1 μs and individual pulse duration as short as 4 ns. The number and spacing of the pulses is quite flexible but is ultimately limited by the ~150 μs period during which the flashlamp-pumped amplifiers have significant gain. The repetition rate of the burst sequence is as high as 10 Hz, limited by the thermal loading of the amplifiers.

The OPO cavity, illustrated schematically in Fig. 1, was designed specifically for use with the burst-mode Nd:YAG pump laser, which differs from typical commercial *Q*-switched Nd:YAG lasers in that the available individual pulse energy at 355 nm is limited to ~30–40 mJ, and the time-averaged spectral linewidth, as will be discussed below, is ~400 MHz. The OPO "gain" medium consists of a pair of 12 mm long type I BBO crystals that are 5 mm × 7 mm in cross section and arranged in a linear cavity configuration. The crystals are oriented to provide walk-off compensation between the pump and signal/idler beams, which provides higher effective gain for the relatively small cross-sectional area (~3 mm diameter) pump beam [15,16]. The cavity employs a broadband high reflector and output coupler coated for 20%–30% reflectivity in the wavelength range of 600–850 nm, which is in between that of the low- and high-finesse cavities employed in the OPO system described in [17]. As will be discussed in detail, this cavity provides feedback at both the signal and idler wavelengths, with round-trip gain, which greatly exceeds the total cavity losses. The 355 nm pump beam is coupled into and out of the cavity using a pair of dichroic mirrors. In some cases the pump beam is retroreflected, producing OPO gain for both direc-

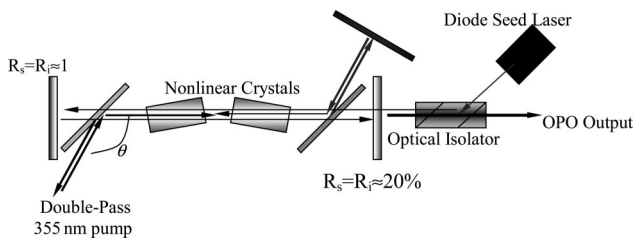

Fig. 1. Schematic of the injection-seeded burst-mode OPO cavity.

tions of signal and idler propagation, which otherwise, due to the phase matching requirement, occurs only in the propagation direction parallel to that of the pump (left to right in Fig. 1). The total cavity length is ~10 cm, limited by the size of the current pump-mirror mounts. The cavity is injection seeded at the idler [12] using a single-frequency external-cavity diode laser (ECDL), two of which, at 780 and 827 nm, are available in our laboratory. In either case, the seed radiation is injected through the output coupler using a Faraday-rotation optical isolator in a manner similar to that employed previously for injection seeding of a titanium:sapphire laser [18].

Single-pass small-signal gain measurements are performed by removing the cavity output coupler and placing a scattering card just after the exit of the optical isolator. The cw ECDL seed-laser beam is passed through the gain medium and retroreflected by the cavity high reflector, as illustrated in Fig. 1. After transmission through the optical isolator, scattering from the card is detected with an ordinary photodiode detector as a function of time with respect to the Nd:YAG pump pulse. An ordinary interference filter is placed just in front of the detector to attenuate stray light from the flashlamp-pumped amplifiers. Note that for these measurements the pump beam is not double passed, so the seed laser only experiences gain during the retroreflected pass through the BBO crystals. Time-dependent small-signal single-pass gain is measured, for a single pulse, as a function of 355 nm pump-pulse energy in the range of 3–18 mJ.

The time-averaged spectral linewidth of the second-harmonic output of the Nd:YAG pump beam is measured with a scanning confocal spectrum analyzer, with 2 GHz free spectral range (355 nm mirrors were unavailable). Instantaneous and time-averaged spectral linewidths of the pulsed OPO signal and idler outputs were measured with a commercial (HyFinesse WS7) Fizeau wavemeter system with a resolution of ~100 MHz. Temporal traces of the signal and idler burst train output are recorded simultaneously with the 355 nm pump using a pair of photodiodes and a digital oscilloscope. Average burst energy is recorded with an ordinary commercial thermopile power meter.

3. Results and Discussion

A. Gain Measurements

For "small-signal" conditions, in which the depletion of the pump wave can be ignored, the single-pass gain, G, for an optical parametric amplifier can be approximated by [9]

$$G = \frac{1}{4}\exp\left(2l\sqrt{\frac{8\pi^2 d_{\mathrm{eff}}^2 I_p}{\lambda_s \lambda_i n_s n_i n_p \varepsilon_0 c}}\right), \qquad (1)$$

where I_p is the intensity of the pump wave, d_{eff} is the nonlinear coefficient of the medium, and l is the path length. Figure 2 shows the natural log of the single-pass gain as a function of the square root of the pump energy, for pump energies between 3 and 18 mJ/pulse. For energies exceeding ~20 mJ, optical feedback from uncoated optical elements resulted in the onset of lasing. It can be seen that the single-pass gain increases logarithmically with the square root of increasing pump energy, as expected from Eq. (1), reaching a value of ~140 at 18 mJ/pulse. Ignoring losses other than the cavity high reflector (20%) and assuming that the gain in each direction is approximately equal when the OPO pump is retroreflected as illustrated in Fig. 1, we estimate a round trip gain of ~4000. In fact, the gain is even higher at the highest pump energies employed (~30 mJ/pulse). As will be demonstrated, the combination of high gain and low cavity finesse results in a simple method for achieving narrow linewidth output at both the signal and idler wavelengths.

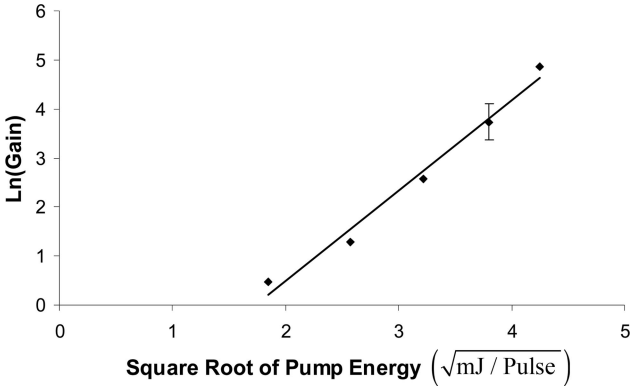

Fig. 2. Small-signal gain versus pump energy with approximate error bars as indicated.

B. Burst-Mode Output Measurements

A series of baseline measurements were performed in which the burst-mode pump laser was operated in a manner identical to that used to generate high-frequency pulse trains but with only a single pulse per burst. The results are summarized in Fig. 3, which shows OPO signal and idler power-conversion

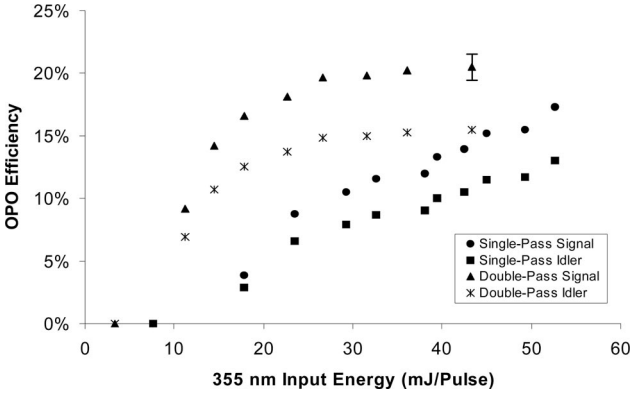

Fig. 3. OPO conversion efficiency as a function of pump energy for single 355 nm pulses from the burst-mode laser with approximate error bars as indicated.

efficiencies as a function of input pulse energy when the OPO cavity is operated in single- and double-pass pump configurations. We note that the data shown in Fig. 3 were obtained for signal and idler wavelengths of 622 and 827 nm, respectively, which were selected due to the availability of an ECDL seed laser for line narrowing, as will be discussed in Subsection 3.C. However, when operated with appropriate high reflector and output coupler cavity optics, we demonstrated essentially identical results for signal wavelengths between ~450 and 710 nm (the degeneracy point for 355 nm pumping), as is typical for a 355 nm pumped BBO OPO [9].

It can be seen that when operated in single-pass mode, threshold occurs at ~8 mJ per pulse, with conversion efficiency increasing relatively slowly and reaching a maximum of ~30% (total signal + idler) at the highest attempted pump energy of 55 mJ. Operation in double-pass mode reduces the OPO threshold by ~50%, from 8 to 4 mJ, and more importantly, results in conversion efficiency, which rises more rapidly as a function of input energy, reaching a plateau of ~35% (total signal + idler) for a pump input energy of 30 mJ. It is important to point out that low threshold, while always important for nonlinear processes, is particularly critical for burst-mode operation of the OPO due to the inherent intensity envelope of the individual pump pulses within the burst. While we have not yet explored this in detail, we note a general guideline for OPO operation, which states that the pump intensity should be a factor of approximately 4 greater than threshold [9].

Operation in burst mode is illustrated in Figs. 4 and 5, which show some typical single-burst sequences for the 355 nm pump (upper trace) and corresponding OPO idler output (lower trace) at 780 nm. Note that signal traces, not shown, are very similar. Also note that due to the limited sampling rate of the digital oscilloscope, an ~10 kΩ load resistor was purposefully employed to enable capture of the burst sequence. The apparent $\sim 10^{-6}$ s decay time of the individual pulses is a consequence of this added resistance. The actual measured individual pulse duration, as will be shown, is ~4 ns. In each of the illustrated cases, the OPO cavity was operated with injection seeding of the idler wave at 780 nm (unseeded operation gave nearly identical pulse energies). Figure 4 illustrates a 6 pulse, 10 μs spacing burst, with average single-pulse pump energy of 31 mJ. Figure 5 shows a 10 pulse, 6 μs spacing burst, with average single-pulse pump energy of 16 mJ. A variety of additional combinations have been produced ranging from 1 to 12 pulses with 4–12 μs spacing. In all cases total signal + idler conversion efficiency is 30% or more, essentially identical to that obtained using a single pulse. It is also noted that the intensity envelopes of the OPO output follow reasonably, but not precisely, the envelopes of the pump pulses, a result that we attribute to pump pulses with intensity significantly above threshold by a factor of 4 or more. In this regard it is important to note that the

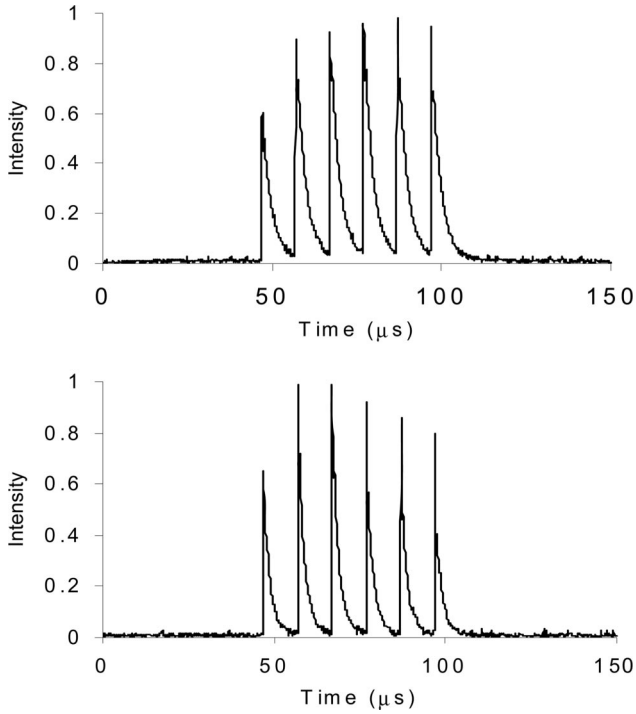

Fig. 4. Typical six-pulse, 10 μs spacing pump (upper) and OPO burst sequence (lower). Total OPO conversion efficiency (signal + idler) is 33%. Average single-pulse 355 nm input energy is 31 mJ.

pump laser produces bursts with an inherent pulse-to-pulse intensity variation, particularly when operated at high intensity for which gain narrowing is significant. The multiple nonlinear steps (second-,

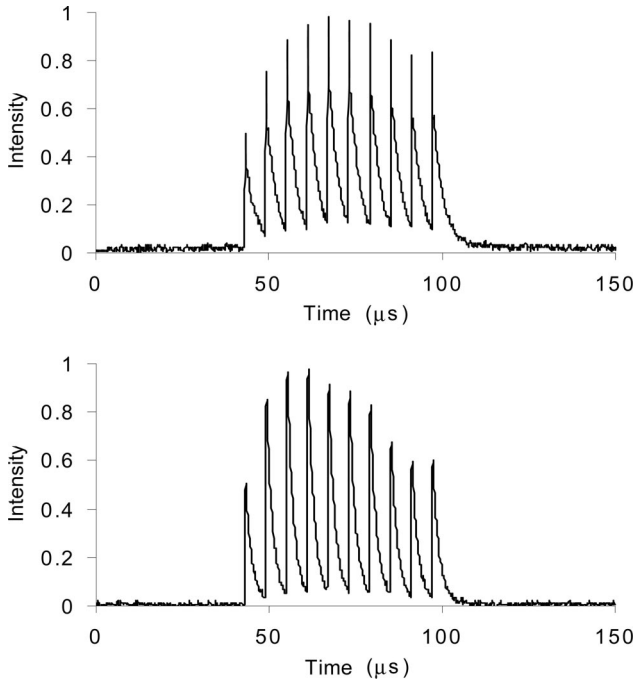

Fig. 5. Typical ten-pulse, 6 μs spacing pump (upper) and OPO burst sequences (lower). Total OPO conversion efficiency (signal + idler) is 32%. Average single-pulse 355 nm input energy is 16 mJ.

third-harmonic followed by OPO) will tend to exacerbate this problem, and so it is critical to produce the most uniform pump bursts as possible.

C. Linewidth and Injection-Seeding Measurements

We have also performed measurements of line narrowing of the signal and idler waves by means of injection seeding. Prior to these measurements, the 355 nm pump linewidth was estimated from linewidth measurements of the second harmonic using a 2 GHz free spectral range confocal spectrum analyzer. While this device is not designed for linewidth measurements of pulsed beams, it can nonetheless provide a reasonable estimate. The spectrum analyzer was scanned slowly using a computer-generated voltage ramp applied to the controller's external ramp input. An ordinary PIN photodiode captured the transmitted signal, which was processed with a boxcar averager and digitized with the computer. Results are illustrated in Fig. 6, which show time-averaged etalon traces measured before (solid curve) and just after (dashed curve) the PCM. Comparison of the two traces clearly illustrates the broadening effect due to the stimulated Brillouin scattering process. Prior to the PCM the apparent time-averaged full width at half maximum (FWHM) at 532 nm, which includes a contribution of less than 20 MHz from the finite finesse (~100) of the etalon, is ~160 MHz. As illustrated in Thurow *et al*. [1], the individual burst-mode pump-laser fundamental (1064 nm) pulses, prior to the PCM, have a duration of ~8.2 ns and are somewhat flat topped in profile, due to the pulse slicer. For a Gaussian temporal profile, the Fourier transform-limited linewidth is given by the well known expression [19]

$$\Delta v_{\mathrm{FWHM}} \Delta t_{\mathrm{FWHM}} = 4 \ln(2)/\pi \approx 0.88. \qquad (2)$$

A very similar linewidth limit, $\Delta v_{\mathrm{FWHM}} \Delta t_{\mathrm{FWHM}} \approx 0.88$, also results from a flat-top, sinc^2 Fourier transform pair [19], so that the Fourier transform-limited linewidth for the 8.2 ns fundamental pulse is ~107 MHz. Assuming the second-harmonic process results in an increase in linewidth by a factor of $\sqrt{2}$, we estimate a minimum linewidth at 532 nm of ~150 MHz, in reasonable agreement with the measurement. Similar agreement was reported by Wu *et al*. [2].

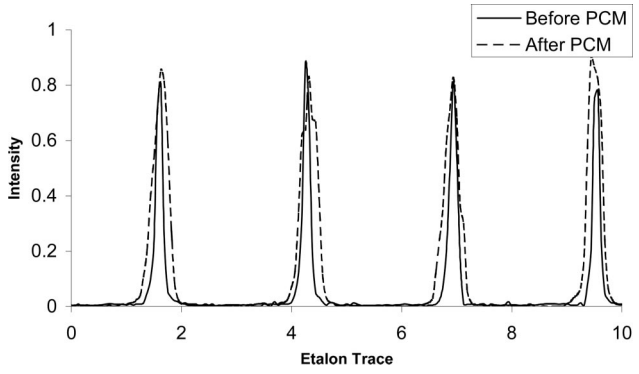

Fig. 6. Etalon trace of second-harmonic (532 nm) output of burst-mode laser before (solid) and after (dashed) the PCM.

From the dashed curve of Fig. 6 it can be seen that the linewidth of the second-harmonic beam at 532 nm increases by a factor of approximately two, to ~320 MHz, as a result of the PCM stimulated Brillouin scattering process. This homogenous line broadening is a consequence of the rapid decay time for the acoustic grating established by the high-intensity stimulated Brillouin scattering (SBS) pump beam. For the fluorinated hydrocarbon used in this work, known commercially as Fluorinert FC-75, the hypersound decay time is ~0.90 ns, corresponding to a measured spontaneous Brillouin scattering linewidth FWHM of 350 MHz [20]. While we have not studied the SBS line broadening in any detail, it is expected, due to line narrowing, that the additional linewidth imparted by the SBS process would be a fraction of the spontaneous Brillouin scattering linewidth [21].

Based on the above measurements, we estimate the time-averaged linewidth for the 355 nm OPO pump to be given approximately by the rms of the linewidths of the fundamental and second-harmonic beams, or ~400 MHz; a value that is a significant fraction of the approximate 1.5 GHz longitudinal-mode spacing of the OPO cavity.

In the absence of injection seeding, time-averaged linewidths of ~1 nm (~439 and 775 GHz at 827 and 622 nm, respectively) are observed for both the signal and idler beams, using a simple grating spectrometer. Figures 7 and 8 illustrate the effect of injection seeding in the time and frequency regimes, respectively. Figure 7(a) shows single-shot oscilloscope time traces for the 355 nm pump beam and the OPO idler beam at 827 nm for operation while unseeded and while seeded at the idler wavelength. Build-up time reduction of ~1 ns is clearly observed for the seeded case, corresponding to approximately one round trip through the 10 cm path-length cavity. Compression of both of the idler pulses to ~4 ns, relative to the rather asymmetric ~6 ns 355 nm pump, is also readily apparent. Figure 7(b) shows the corresponding time-domain traces for the OPO signal beam at 622 nm, where again the cavity has been injection seeded at the 827 nm idler wavelength. Build-up time reduction of ~1 ns is again observed.

Figure 8 shows representative interference patterns obtained with a commercial dual wedge Fizeau wavemeter (HyFinesse Model WS7) of a single OPO signal output pulse at 622 nm when the cavity is seeded at the idler wavelength of 827 nm with a cw ECDL. The idler beam interference patterns, not shown, are essentially identical. For both the signal and idler outputs, individual pulse linewidth values, as determined by the wavemeter, oscillated randomly between 200 and 300 MHz, with most values being equal to 300 MHz. Referring to Eq. (2) we note that the predicted Fourier transform limit corresponding to 4 ns FWHM duration Gaussian pulses is ~220 MHz, in good agreement with the observations. We stress that the observed line narrowing of both

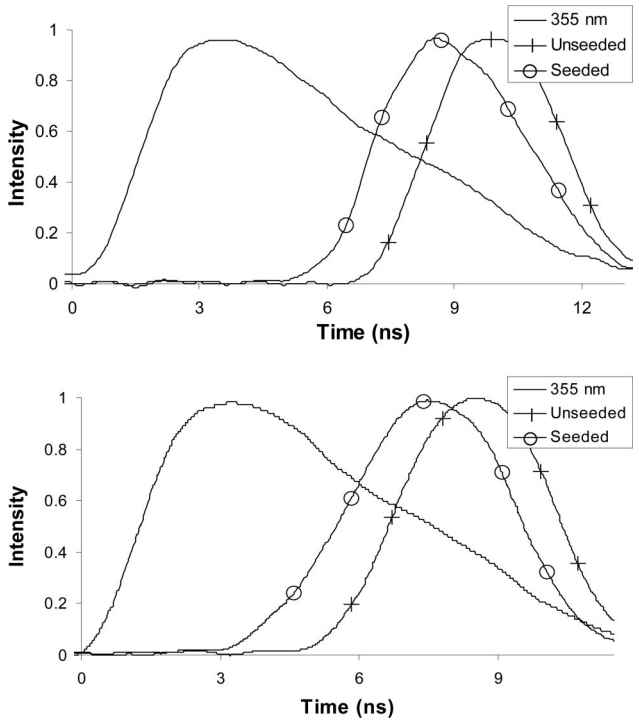

Fig. 7. Time traces of pump (solid), seeded (circles), and unseeded (crosses) OPO output illustrating build-up time delay. Upper and lower traces correspond to 827 nm idler and 622 nm signal wavelengths, respectively. Seeding is at the idler wavelength.

the signal and idler beams was achieved without any active stabilization of the OPO cavity length to match the seed wavelength.

To understand this result we note several features of the burst-mode OPO cavity. First the cavity has

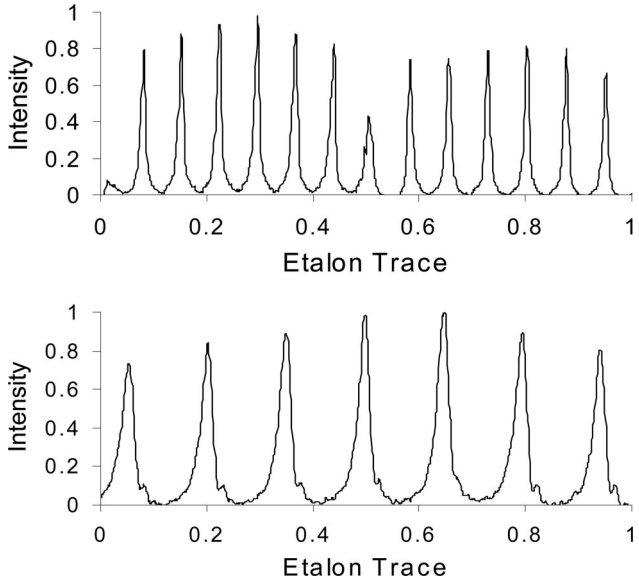

Fig. 8. Dual wedge Fizeau wavemeter interference patterns for single OPO signal pulse when cavity is seeded at the idler wavelength with a cw ECDL. Upper and lower traces correspond to low and high resolution Fizeau wedge, respectively. Idler pulse output is essentially identical.

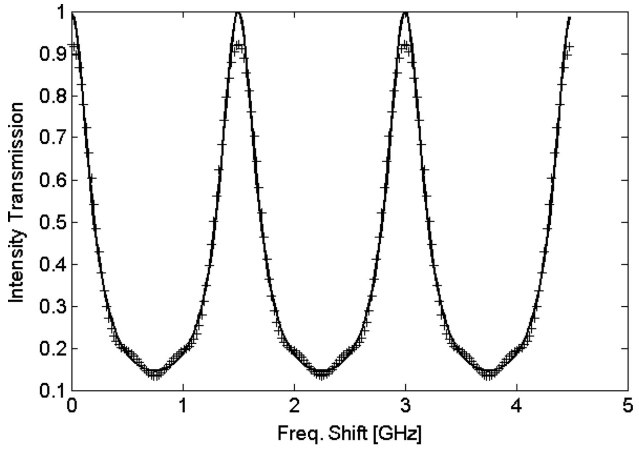

Fig. 9. Airy function (solid) for OPO cavity used in this work, illustrating minimum transmission of 15%. Symbols correspond to Eq. (3), truncated at $n = 4$.

quite low finesse. Figure 9 (solid) shows a computed Airy function for a cavity with a 20% reflectivity output coupler (by power) and 100% reflectivity high reflector. It can be seen that the "transmission" is never less than ~15%, whereas the round-trip small-signal gain, ignoring the output coupler loss but including distributed cavity losses of ~30% (mostly from the uncoated BBO crystal surfaces), exceeds 15,000 assuming a single-pass small-signal gain of ~150 (see Fig. 2). Clearly, in some sense, the cavity can be thought of as a multipass amplifier, although the net gain is affected, at some wavelengths more than others, by partial field cancellation due to multiple beam interference. It is also possible, although it has not been explored, that the idler output frequency is "pulled" somewhat from the seed, occurring at a frequency closer to a cavity longitudinal mode maximum. Second, the ~400 MHz linewidth of the 355 nm pump is a significant fraction of the 1.5 GHz longitudinal mode spacing. This facilitates meeting the energy-conservation requirement for narrow-linewidth output at the signal wavelength. Finally, we note that we have not attempted to scan the seed laser continuously. The fringe patterns shown in Fig. 8 were obtained by coarsely adjusting the BBO crystal angles while monitoring the spectral output at low resolution using a grating spectrometer. While the purpose was to adjust the OPO gain profile to match the idler seed approximately, angular tuning of the crystals also affects the effective cavity path length. Diagnostic experiments involving continuous tuning of the seed laser are planned for the near future.

While not critically important, it is worthwhile to recall that the Airy function results from the geometric series convergence of an "infinite" number of interfering coherent beams [22]:

$$E_t = E_o t^2 \sum_{n=0}^{\infty} r^{2n} e^{in\phi}, \tag{3}$$

where n is the beam index, $r = \sqrt{r_{OC} r_{HR}}$ is the effective reflectivity of the cavity, in terms of electric field, t is the field transmission, and φ is the phase angle corresponding to the propagation of the field through one cavity round trip. For a short pulse the number of interfering beams is clearly limited. For example, a pulse duration of 4 ns corresponds to approximately six interfering beams, assuming a 20 cm cavity round-trip length. The "+" trace in Fig. 9 shows the computed transmission as a function of phase angle from Eq. (3) for the case where the index n has been truncated at 4. While some deviation from the full Airy function is observed, particularly at the transmission peaks and in the vicinity of the intermode minima, the overall differences are small. For six interfering beams, not shown in Fig. 9, the difference is very difficult to discern on a linear scale.

4. Conclusions

The ability to generate ultra-high-frequency sequences of broadly wavelength-tunable, high-intensity laser pulses using a custom-built injection-seeded OPO pumped by the third-harmonic output of a burst-mode Nd:YAG laser has been experimentally demonstrated. For typical burst sequences, consisting of 6–10 pulses separated in time by between 6 and 10 μs, total signal plus idler conversion efficiency as high as ~35% is obtained, when the 355 nm pump beam is retroreflected through the linear cavity to provide gain in both directions of beam propagation. This corresponds to typical individual pulse energies, for the signal or idler beams, of ~6.0 mJ, limited by available pump power.

Line narrowing of both the signal and idler beams, from ~1 nm to ~300 MHz, is demonstrated by means of cw injection seeding, with a commercial ECDL at the idler wavelength. Line narrowing is achieved without recourse to cavity stabilization, which is believed to be due to a combination of the rather low finesse and high gain of the OPO cavity, and utilizing a 355 nm pump linewidth of ~400 MHz, which is a significant fraction (~25%) of the cavity longitudinal mode spacing.

Immediate future work will focus on the generation of tunable ultraviolet (UV) output in the vicinity of 226 nm, enabling ultra-high-frame-rate PLIF imaging of NO. The required UV wavelength will be generated from the OPO output by means of sum-frequency mixing of the signal, at 622 nm, with residual 355 nm pump energy. Individual pulse energy at 226 of ~1–2 mJ is anticipated, dependent upon anticipated increases in available 355 pump power. Significant extension of the burst envelop will also be attempted, using long-pulse-duration power supplies for pumping the Nd:YAG amplifier chain. Preliminary work has indicated that this approach can generate high energy, up to ~400 mJ/pulse at 1064 nm, bursts of ~20 pulses at 50 μs spacing (20 kHz). It is anticipated that such sequences will be used for OH PLIF imaging in subsonic turbulent combustion systems in the near future.

The authors thank Brian Thurow, currently of Auburn University, for his assistance and many useful discussions during his tenure in the Ohio State Gas Dynamics Laboratory. The support of the Air Force Research Laboratory Propulsion Directorate Small Business Innovation Research Program under contract F33615-03-C-2339 is acknowledged, as well as support from the National Science Foundation, Division of Chemical and Transport Systems.

References

1. B. Thurow, N. Jiang, M. Samimy, and W. Lempert, "Narrow-linewidth megahertz-rate pulse-burst laser for high-speed flow diagnostics," Appl. Opt. **43,** 5064–5073 (2004).
2. P. Wu, W. R. Lempert, and R. B. Miles, "MHz pulse-burst laser system and visualization of shock-wave boundary-layer interaction in a Mach 2.5 wind tunnel," AIAA J. **38,** 672–679 (2000).
3. K. Kohse-Hoinghaus and J. B. Jeffries, *Applied Combustion Diagnostics* (Taylor & Francis, 2002).
4. P. M. Danehy, J. A. Wilkes, D. W. Alderfer, S. B. Jones, A. W. Robbins, D. P. Patry, and R. J. Schwartz, "Planar laser-induced fluorescence (PLIF) investigation of hypersonic flowfields in a Mach 10 wind tunnel," presented at the 25th AIAA Aerodynamic Measurement Technology and Ground Testing Conference, San Francisco, Calif., 5–8 June 2006, paper AIAA-2006-3442.
5. P. M. Danehy, S. O'Byrne, A. F. P. Houwing, J. S. Fox, and D. R. Smith, "Flow-tagging velocimetry for hypersonic flows using fluorescence of nitric oxide," AIAA J. **41,** 263–271 (2003).
6. P. Wu, W. R. Lempert, and R. B. Miles, "Tunable pulse-burst laser system for high-speed imaging diagnostics," presented at the 36th AIAA Aerospace Sciences Meeting, Reno, Nev., 12–15 January 1998, paper AIAA-98-0310.
7. J. D. Luff, D. K. Mansfield, S. H. Zaidi, H. Aschoff, J. W. Kuper, and R. B. Miles, "Development of a tunable megahertz pulse-burst alexandrite laser system," presented at the 34th AIAA Plasmadynamics and Lasers Conference, Orlando, Fla., 23–26 June 2003, paper AIAA-2003-3746.
8. C. F. Kaminski, J. Hult, and M. Alden, "High repetition rate planar laser induced fluorescence of OH in a turbulent non-premixed flame," Appl. Phys. B **68,** 757–760 (1999).
9. W. Koechner, *Solid-State Laser Engineering,* 4th ed. (Springer-Verlag, 1992).
10. J. E. Bjorkhom and H. G. Danielmeyer, "Frequency control of a pulsed nanosecond optical parametric oscillators by radiation injection," Appl. Phys. Lett. **15,** 171–173 (1969).
11. D. C. Hovde, J. H. Timmermans, G. Scoles, and K. K. Lehmann, "High power injection seeded optical parametric oscillator," Opt. Commun. **86,** 294–300 (1991).
12. J. A. J. Fitzpatrick, O. V. Checkhlov, J. M. F. Elks, and C. M. Western, "An injection seeded narrow bandwidth pulsed optical parametric oscillator and its application to the investigation of hyperfine structure in the PF radical," J. Chem. Phys. **115,** 6920–6930 (2001).
13. A. Y. Dergachev, B. Pati, and P. F. Moulton, "Efficient third-harmonic generation with a Ti:sapphire laser," in *Advanced Solid State Lasers,* M. Fejer, H. Injeyan, and U. Keller, eds., Vol. 26 of OSA Trends in Optics and Photonics (Optical Society of America, 1999), paper PD3.
14. C. K. Ni and A. H. Kung, "Effective suppression of amplified spontaneous emission by stimulated Brillouin scattering phase conjugation," Opt. Lett. **21,** 1673–1675 (1996).
15. D. J. Armstrong, W. J. Alford, T. D. Raymond, A. V. Smith, and M. S. Bowers, "Parametric amplification and oscillation with walkoff-compensating crystals," J. Opt. Soc. Am. B **14,** 460–474 (1997).
16. W. R. Bosenberg, W. S. Pelouch, and C. L. Tang, "High-

efficiency and narrow-linewidth operation of a two-crystal β-BaB_2O_4 optical parametric oscillator," Appl. Phys. Lett. **55,** 1952–1954 (1989).
17. W. D. Kulatilaka, T. N. Anderson, T. L. Bougher, and R. P. Lucht, "Development of injection-seeded, pulsed optical parametric generator/oscillator systems for high-resolution spectroscopy," Appl. Phys. B **80,** 669–680 (2005).
18. W. Lee and W. Lempert, "Enhancement of spectral purity of injection-seeded titanium:sapphire laser by cavity locking and stimulated Brillouin scattering," Appl. Opt. **42,** 4320–4326 (2003).
19. R. N. Bracewell, *The Fourier Transform and Its Applications,* 2nd ed. (McGraw-Hill, 1986).
20. H. Yoshida, V. Kmetik, H. Fujita, M. Nakatsuka, T. Yamanaka, and K. Yoshida, "Heavy fluorocarbon liquids for a phase-conjugated stimulated Brillouin scattering mirror," Appl. Opt. **36,** 3739–3744 (1997).
21. A. L. Gaeta and R. W. Boyd, "Stochastic dynamics of stimulated Brillouin scattering in an optical fiber," Phys. Rev. A **44,** 3205–3209 (1991).
22. W. T. Silfvast, *Laser Fundamentals,* 2nd ed. (Cambridge U. Press, 2004).